Self-Exchange of Polyelectrolyte in Multilayers: Diffusion as a Function of Salt Concentration and Temperature

*Rachel L. Abbett, Yuhui Chen, Joseph B. Schlenoff**

Department of Chemistry and Biochemistry, Florida State University, Tallahassee, FL 32306, U.S.A.

Accepted Version *Macromolecules* 2021

*jschlenoff@fsu.edu

ABSTRACT

Polymer chain diffusion within a hydrated polyelectrolyte complex, PEC, has been measured using an ultrathin film format prepared by the layer-by-layer method. Isotopically-labeled self-exchange of deuterated poly(styrene sulfonate), dPSS, with undeuterated PSS of the same narrow molecular weight distribution permitted reliable estimates of whole-molecule diffusion coefficients, D. Narrow molecular weight distribution poly(diallyldimethylammonium), PDADMA, was used as the polycation for the PEC. Extensive pretreatment of starting films was undertaken to remove residual stress, anisotropy and layering. PSS/PDADMA "multilayers", PEMUs, thin enough to provide substantial exchange of polyelectrolyte, even with diffusion coefficients as low as 10^{-16} cm^2 s^{-1}, as a function of salt concentration and temperature were measured for this PEC, which has a glass transition temperature, T_g, close to room temperature. Two molecular weights of d-PSS, about 15 kDa and 100 kDa, presumed to be below and above the entanglement molecular weight, respectively, both diffused faster at higher temperatures with respective activation energies, E_a, of about 21 and 53 kJ mol^{-1}, the latter about the same as E_a for the place exchange between two pairs of PSS:PDADMA. Studies of the linear viscoelastic response of macroscopic PECs showed a difference of about 8 ^oC in the T_g of the two lengths of PSS complexed with the same PDADMA. Increasing concentrations of NaCl influenced D of 100 kDa PSS but not 15 kDa PSS at room temperature. D was faster in the region of film near the solution interface, again attributed to a lower T_g caused by greater water content at this interface.

Introduction

The layer-by-layer, LbL, assembly of polyelectrolyte multilayers (PEMUs) to produce ultrathin films has been explored extensively over the past few decades.[1, 2, 3] This method of making films is a versatile approach to producing thin composite materials with short-range control over the composition at the nanoscale.[4, 5, 6, 7, 8, 9] Because the ratio of polyelectrolyte components can be adjusted[1, 10] the film can be tailored to specific applications, such as "reservoirs."[11] PEMUs have also been considered for drug delivery systems,[11, 12] cell sheet engineering,[13] as well as electronic and optical devices[14] such as LEDs, solar cells,[15] and sensors[16] due to the tunability of the total excess charge of the system. Selective transport of ions and water through PEMUs suggests their use as water purification membranes.[17]

PEMUs often contain an excess of one of the polyelectrolyte components, termed "overcompensation." Overcompensation is a result of the sequential method of LbL assembly.[18] The extent of overcompensation is thought to be caused by differences in charge density, hydrophobicity, and diffusion coefficients between polyelectrolytes.[1, 6, 10, 19, 20, 21, 22, 23] It is possible to tune the degree of overcompensation through variables such as exposure time and salt concentration during build-up or by annealing films with salt post assembly.[18]

Contrary to the implications of most simplified cartoons, including those used here, PEMUs from polyelectrolytes do not form in discreet layers but actually intermix so that positive polyelectrolyte repeat units, Pol^+, can pair with negative units, Pol^-, yielding a less ordered "scrambled salt."[24] Both the polyelectrolyte molecules themselves[25, 26, 27] and the Pol^+ or Pol^- sites compensated by counterions ("extrinsic sites") are able to move throughout the film.[28] Distinguishing between the diffusion of sites versus polyelectrolyte molecules can be a challenge. Both are controlled by the salt concentration and temperature [27, 28, 29, 30] as well as film thickness.[26, 31, 32]

PEMUs have similar, but more stratified, compositions to "complexes" or "coacervates," PECs, made by mixing the same polyelectrolytes in solution.[33] The ultrathin film format of PEMUs lends itself well to studying polyelectrolytes that slowly diffuse only a short distance in a long time. Most of the methods for observing polyelectrolyte diffusion in a PEMU rely on some kind of label. For example, a deuterated layer included within many protiated layers can be tracked using neutron reflectivity.[25, 27, 34] The spread of neutron contrast with time is unequivocally due to redistribution of labeled polyelectrolyte within the film. However, once the deuterated layer diffuses about a coil diameter it can no longer be seen, as it becomes diluted by unlabeled polyelectrolyte. An early study of the diffusion of deuterated poly(styrene sulfonate), dPSS, layers in a PEMU of PSS and poly(diallyldimethylammonium), PDADMA, considered the spreading of dPSS layers on exposure to a solution of high NaCl concentration using neutron reflectometry.[27] It took many hours for a 5 nm "layer" of dPSS to diffuse another 10 nm at room temperature. Small angle neutron scattering later showed the same molecular weight dPSS (10^5 g mol^{-1}) in thoroughly equilibrated/annealed PDADMA/PSS PEC to have radius of gyration, R_g, of about 10 nm, suggesting the dPSS absorbs in a slightly flattened conformation.[35]

A reliable method of measuring diffusion through bulk medium employs self-exchange of unlabeled versus labeled molecules. If a film is at least several polymer coil diameters in thickness and the polymer can access most or all of the film, there is no doubt that one is observing molecule-scale diffusion during self-exchange.[36] Lavalle et al. were the first to demonstrate self-exchange of (fluorescently labeled) polyelectrolytes from a PEMU.[37] Isotopic self-exchange of dPSS for protiated PSS (hPSS) was demonstrated by our group several years later.[28]

Much has been learned about the vast differences in molecule dynamics for PECs of different composition. For example, the bulk properties of PEMUs investigated by the Strasbourg group, made from polypeptides,[38, 39] fall into the liquidlike or "coacervate" category, whereas PDADMA/PSS is actually glassy at room temperature, with a glass transition temperature, T_g

around 35 °C, whether as an ultrathin film[40] or in bulk PEC.[41] Polymers locked into glassy systems are expected to diffuse exceptionally slowly, as found for PDADMA/PSS.

Glass transitions are not uncommon in complexed polyelectrolytes.[42] As with any glassy polymer, heating through the T_g results in a marked drop in modulus. It is of interest to evaluate the response at T_g of the various components that make up the PEMU or PEC. For example, no or minimal transitions were observed in the rate of diffusion of salt (Na^+ Cl^-) ions or water as PDADMA/PSS passed though T_g.[43] Because the diffusion coefficient of polyelectrolyte components is orders of magnitudes slower, in the present work we focus on the response of polymer diffusion to changes in both temperature and salt concentration. Isotope self-exchange of dPSS by hPSS was employed, using FTIR to track the clear changes in deuterium content as a function of time.

Materials and Methods

Materials: Poly(diallyldimethylammonium chloride) (molar mass, MM, 200,000-250,000 g mol^{-1}) was from Sigma-Aldrich and fractionated as described previously to give M_w = 70,000, PDADMAC.[44] Two chain lengths of poly(styrene sulfonate) are denoted as "short chain" (S-PSS) and "long chain" (L-PSS). Deuterated poly(styrene sulfonate) with M_w =104,000, L-dPSS, and M_w 14,000, S-dPSS, were matched with protiated poly(styrene sulfonate) (M_w 104,000, L-hPSS), made from polystyrene as described by Coughlin et al.[45] The level of initial deuteration varied between samples because the polymers were sulfonated with either D_2SO_4 or H_2SO_4. Polystyrene sulfonated with H_2SO_4 resulted in replacement of about half of the aromatic -D with -H.[45] S-hPSS (M_w = 16,000) was obtained from Scientific Polymer Products. Deionized water (18.2 MΩ cm, Barnstead, Nanopure Diamond) was used to prepare all solutions.

Polymer	**M_w**	**M_n**	**M_w/ M_n**
S-dPSS (deuterated)	14,000	13,800	1.01
S-hPSS	16,000	14,200	1.13
L-dPSS (deuterated)	104,000	103,100	1.01
L-hPSS	104,000	103,300	1.01
PDADMA	70,000	61,600	1.13

Table 1. Molar masses and polydispersities of polymers studied.

Preparation of PEMUs: The polyelectrolyte multilayers were prepared using a robot to perform the alternating addition of polycations and polyanions. The multilayers were made with either high or low molecular weight PSS relative to one another. 2 mM solutions of either L-dPSS or S-dPSS in 1.0 M NaCl were layered with 2 mM solutions of PDADMA in 1.0 M NaCl on double side polished Si (100) wafers. The substrates were exposed to the polymer solutions for 10 minutes per addition, with three 1-minute water rinses between layers, for a total of 20 layers for the L-dPSS samples and 40 layers for the S-dPSS samples to produce similar thicknesses. After the final layer, the films were soaked in the corresponding dPSS solution for 4 h to overcompensate the film with dPSS.[18] The samples were then rinsed 3 times for 1 min in water and dried under a gentle stream of nitrogen. The thickness of each sample was measured with an ellipsometer and the samples were annealed for 24 h in 1.0 M NaCl. The samples were then left in the same salt solution and heated for one hour at 45 ºC before being rinsed briefly in water and dried under nitrogen. This procedure ensured all films were thoroughly annealed and equilibrated, had no residual "fuzzy" layering[9] and no residual stresses or anisotropies before the exchange experiments.

Thickness measurements: Thicknesses of dry films were measured using a Gartner Scientific L116 S ellipsometer set at 70 degrees angle of incidence on Si wafers with a refractive index of 3.85, and the sample refractive index set to 1.55 for PDADMA/PSS systems. Measurements were taken before and after PSS exchange to verify that there was no net material loss during exchange. A standard to convert the FTIR absorption peak area at 1185 cm^{-1} to film thickness was prepared by depositing 10 layers of PDADMA/PSS from 1.0 M NaCl on double side polished silicon wafer and overcompensating with PSS as above. The dry thickness was measured to be 92 nm. The 1185 cm^{-1} band (SO_3^- antisymmetric vibration) does not change during the experiment. It is known that PDADMA/PSS PEC has a water content of about 40 wt% in aqueous solution between 0 and 1.25 M NaCl.[46] Using the density of pure PDADMA/PSS of 1.26 g cm^{-2}, this water content represents half of the volume. Thus, all dry thicknesses were doubled for diffusion calculations (i.e. diffusion coefficients are for the fully hydrated materials).

FTIR measurements: Transmission FTIR measurements were recorded on a Nicolet Avatar 360 FTIR on the Si wafers. Spectra were taken with a dry air purge with 100 scans at a resolution of 4 cm^{-1}. Vibrational bands used to determine the amount of remaining deuterated were the 1090 cm^{-1} band characteristic of the deuterated PSS, which was assigned to the in-plane skeleton vibration of the benzene ring, significantly shifted from the same mode in hPSS (at 1130 cm^{-1}) and the large band at 1185 cm^{-1}, which showed almost no change in shape and intensity and was thus used as an internal standard (Supporting Information Figure S1). The ratio of the 1090 cm^{-1} peak area to the 1185 cm^{-1} peak area was used as a measure of concentration. Identical samples were prepared using protiated PSS for comparison (see Supporting Information, Figure S1 for a comparison of pure hPSS, dPSS, and multilayers with hPSS and dPSS).

Heating control: Temperatures were maintained to ± 0.1 ºC using a Polystat recirculating water bath (Cole-Parmer). Samples were submerged in exchange solutions of 2 mL 10 mM hPSS in 20 mL scintillation vials that were sealed and maintained in the water bath. Solutions were pre-heated or cooled in the bath for 10 minutes prior to sample exposure.

Exchange/Diffusion measurements: Sample thickness and initial dPSS content were measured via FTIR. Each sample was then placed into a solution containing hPSS at a specified [NaCl] and temperature. After a specified amount of time, the sample was removed, rinsed for ten seconds in water, and dried under a gentle stream of nitrogen. Transmission FTIR measurements were taken of the sample, and the process was repeated for the next time point (see Supporting Information figures S2 - S5 for spectra stacks). It was assumed that all polymer motion was “frozen” when the PEMU was dry.

Rheology: Glass transition temperatures were measured using a TA Instruments Discovery HR-3 hybrid rheometer. Polyelectrolyte complex (PEC) samples were prepared by simultaneously mixing 0.125 M hPSS (high or low MM) and 0.125 M PDADMA in 0.25 M NaCl. The PEC was mixed for 24 hours (the first 12 hours at 60 °C for the L-hPSS samples) to allow full complexation and intermixing. The samples were then rinsed in DI water to remove excess salt. Samples were soaked in 0.1 M NaCl, then pressed using a steel die into 8 mm diameter discs, approximately 3 mm thick, for rheological analysis: the high molecular weight sample was pressed at 60 ºC and the low molecular weight sample was pressed at room temperature. Once pressed the samples were exposed to 0.1, 0.5, 0.75, 1.0, and 1.25 M NaCl for 12 h prior to rheology at each salt concentration. A reservoir was used to enclose the bottom geometry. The samples were placed in the reservoir with desired concentrations of NaCl solution, and the upper geometry was lowered to apply a constant 0.2 N axial force on the samples to prevent sample slip. Strain sweep experiments were carried out to make sure all responses were within the linear viscoelastic region. Temperature sweeps were then performed from 0 to 60 ºC at an oscillation frequency of 0.1 Hz.

Results and Discussion

Self-exchange of isotopically labeled (deuterated) PEMU dPSS for aqueous phase hPSS was employed to evaluate diffusion limited transport of PSS molecules in the z-direction (perpendicular to the substrate), illustrated by Scheme 1.

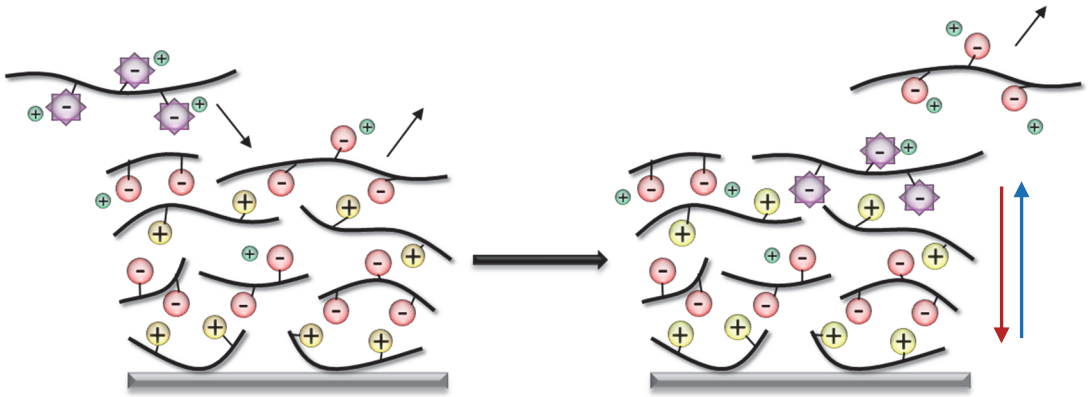

Scheme 1. Depiction of exchange. Protiated hPSS (purple stars), exchanges with deuterated dPSS (red spheres) at the surface and diffuses into the film (red arrow) while deuterated dPSS diffuses out (blue arrow). The rate limiting step for exchange is diffusion within the film and not exchange at, or transport to, the surface. PDADMA (yellow spheres) remains in the film while counter ions (green) compensate excess charge.

Diffusion through a PEMU depends on many variables, primarily temperature, salt concentration, and chain length. Two chain lengths having degrees of polymerization of about 70 and about 500 were considered to be below and above the length for entanglement, respectively. A related PEC system with slightly more water was estimated to have 343 repeat units at the entanglement point.[47] Film thickness was generally held between 500 and 800 nm for direct comparison of the different systems. The thickness of each deposition step in these systems depended on chain length, so the number of layers applied to the substrate was adapted for the two systems so that they would be of comparable thicknesses. The extensive overcompensation and annealing applied to each starting film before exchange is expected to remove any traces of "fuzzy" layering.[9]

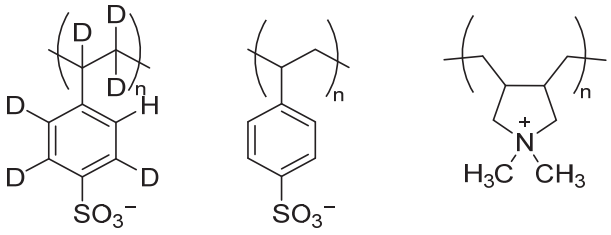

d-PSS PSS PDADMA

Figure 1. Structures for partially deuterated polystyrene sulfonate (dPSS), polystyrene sulfonate (hPSS), and polydiallyldimethylammonium (PDADMA).

Sill et al. studied how the molecular weight of the polycation, PDADMA in a PDADMA/PSS multilayer, altered the diffusion coefficient of the polyanion in the system.[32] It was shown that by varying the build-up conditions and molecular weight of the polycation, the diffusion coefficient of the polyanion could be changed up to 5 orders of magnitude when the polyanion molecular weight is held constant.[32] For this reason, in the current work the PDADMA was carefully fractionated to

provide a narrow polydispersity material (M_w/M_n = 1.13, compared to M_w/M_n ~3 for the starting commercial sample) with a degree of polymerization similar to that of the long PSS molecules. The extensive annealing (in both salt and increased temperature) performed here ensured the ultrathin layer of PDADMA/PSS complex was homogeneous and retained no "memory" of the layer-by-layer assembly.

FTIR transmission spectra on PEMUs supported on double-side-polished Si wafer (transparent in the IR region of interest) enabled clear differentiation of dPSS and hPSS. Spectra were leveled by applying a ramp baseline correction such that absorbances at 970 cm^{-1} and 1770 cm^{-1} were zero. Pure component spectra are provided in the Supporting Information (Figure S1). Assignments for each vibration band, taken from Yang et al.,[48] are summarized in Table 2.

Table 2. Peak assignments for dPSS and hPSS and integration limits used to measure peak area[a]

Wavenumber cm^{-1}	Vibrational mode	Integration Limits cm^{-1}
1010	Aromatic In-Plane Bending	-
1042	SO_3^- Symmetric Vibration	-
1090	Aromatic In-Plane Skeletal Vibration (in dPSS)	1070-1110
1130	Aromatic In-Plane Skeletal Vibration (in hPSS)	-
1185	SO_3^- Antisymmetric Vibration	1140-1270

[a]Assignments following Yang et al.[47]

The dPSS aromatic in-plane skeletal vibration (1090 cm^{-1}) is shifted enough to lower frequency compared to the same mode for hPSS (1130 cm^{-1}) to provide two well-resolved peaks for dPSS and hPSS. Figure 2 shows that the dPSS peak does not overlap with any other peaks. The peak at 1185 cm^{-1} was used as an internal standard and also to provide the dry thickness of the sample. Isotope labeling eliminates the need for a molecular tag that could interfere with the diffusion of the molecules. Baselines were drawn between the integration limits in Table 2 and peak areas normalized to the band at 1185 cm^{-1}.

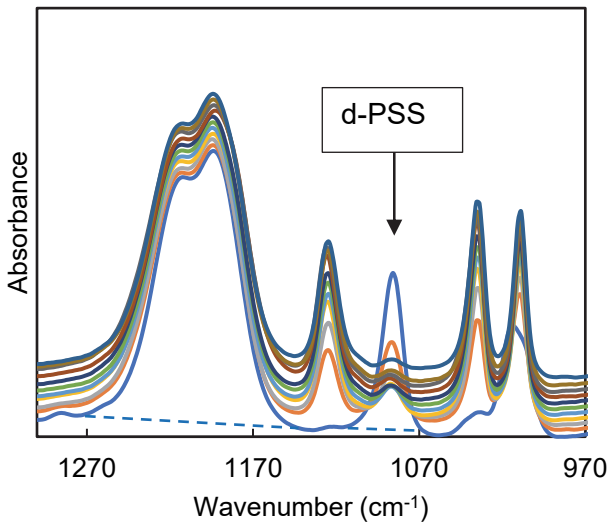

Figure 2. FTIR spectra showing the exchange of deuterated S-dPSS with S-hPSS in 1.0 M NaCl and at 50 °C. All bands are normalized to the band at 1185 cm^{-1}. Baselines for peak integrations are shown as dotted lines. Spectra are stacked for clarity with the t = 0 trace at the

bottom, and time increasing further up the y-axis. The bands from 1270 to 1170 cm^{-1} are not influenced by the exchange and are used as a reference. Dry thickness of film was 606 nm, wet thickness 1212 nm.

Diffusion modeling. Exchange was monitored by the decrease in the 1090 cm^{-1} peak relative to the 1185 cm^{-1} peak in the FTIR spectra. The fraction of remaining dPSS in the film was determined from the spectra. The appropriate equation for describing exchange into/out of a film from one side, limited by finite diffusion in the film is as follows:[49]

$$f = 1 - \frac{C_t}{C_0} = 1 - \sum_{n=0}^{\infty} \frac{8}{(2n+1)^2\pi^2} \exp\left[\frac{-D(2n+1)^2\pi^2 t}{4l^2}\right] \rightarrow \frac{2\sqrt{Dt}}{l\sqrt{\pi}} \; for \; f < 0.7 \qquad [1]$$

where *f* is the fraction of polymer exchanged, C_t is the average concentration of dPSS in the film at time t, C_0 the average concentration of dPSS at t = 0, D is the film diffusion coefficient, t is time in seconds, *l* is the thickness of the film in cm, and n is an integer. The boundary conditions for Equation 1 assume there is negligible dPSS at the surface of the multilayer or in the bulk solution at any time. These boundary conditions were maintained by the facts that D in the film was orders of magnitude lower than D in solution (ca. 10^{-7} cm^2 s^{-1}) and the amount of protiated polymer was >1000 times the amount of deuterated polymer in each experiment. For fractions exchanged up to 0.7 the semi-infinite approximation of Equation 1, given on the right, is valid.

The peak area of the 1090 cm^{-1} deuterated mode (A_D) was normalized to the peak area of the 1185 cm^{-1} peak (A_R) (common to both dPSS and hPSS and unaffected by deuteration) (see Supplemental Information Figures S6-S9).

$$\frac{C_t}{C_0} = \frac{(A_D/A_R)_t}{(A_D/A_R)_0} \qquad [2]$$

Where $(A_D/A_R)_t$ is the ratio at time t, and $(A_D/A_R)_0$ is the ratio at t = 0. It was assumed that at infinite time all the dPSS would diffuse out of the system and be replaced with hPSS. In the cases where the data deviated from the modeling prior to a fraction of 0.6, two fitted diffusion coefficients were used (D1 and D2). For both D1 and D2, C_∞ was still set to $C_t = 1$. For D2, $(A_D/A_R)_0$ was set to where the second diffusion stage begins (see Supplemental Information Table S1) instead of being at t = 0 as it is for D1. This is because the diffusion associated with D2 does not begin until the material has already diffused through the region associated with D1.

Dependence of D on Temperature

Diffusion through a polymer is assumed to depend on whether the sample is above or below the glass transition temperatrue. A known T_g at different salt concentrations is needed for this analysis. Bulk samples of complexed PDADMA and hPSS (high and low molecular weight) were pressed into a disc and dynamic mechanical thermal analysis (DMTA) was used to determine T_g (see Supporting Information Figures S11 and S12 for examples).

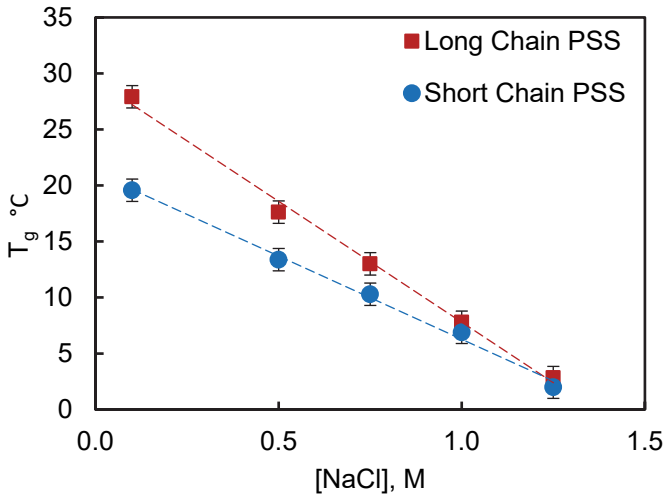

Figure 3. Glass transition temperatures of complexes made with L-hPSS (■) and S-hPSS (●) in different salt concentrations. Measured at 0.1 Hz, with temperature sweeps from 0 to 60 ºC.

The samples experienced a decrease in T_g with increasing salt concentration (Figure 3). The T_g of short chain PSS was lower than that of the long chain PSS, the first observation, to our knowledge, of a T_g dependence on molecular weight in PECs.

The exchange of L-dPSS by L-hPSS was monitored at 10, 20, 30, 40, 50, 60, and 70 ºC in 1.0 M NaCl, where the lowest temperatures were near the T_g's shown in Figure 4. The rate of polymer diffusion for L-hPSS (see Figure 4) decreased with decreasing temperature, with a faster decrease near T_g. The Arrhenius plot of lnD versus 1/T in Figure 4B showed an activation energy of about 53 kJ mol^{-1} above T_g and 98 kJ mol^{-1} below T_g. The former is about the same activation energy as that deduced for the rearrangement of a pair of Pol^+Pol^- associated polyelectrolyte repeat units.[47] This is consistent with the hypothesis that polyelectrolyte chains complexed together move by rapid exchange interactions between pairs of neighboring Pol^+Pol^- units.

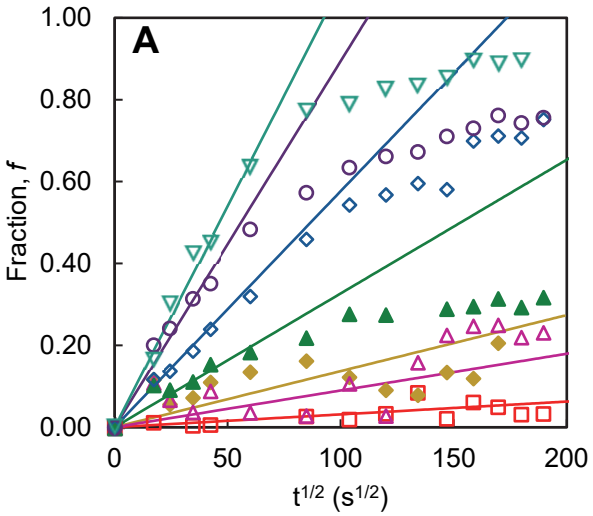

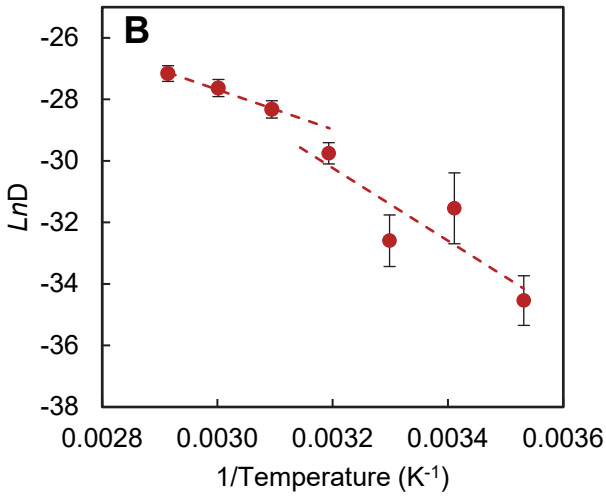

Figure 4. Exchange of L-dPSS by L-hPSS in a PEMU with increasing temperature (**A**); 10 ºC (□), 20 ºC (♦), 30 ºC (△), 40 ºC (▲), 50 ºC (◊), 60 ºC (p○), and 70 ºC (▽). NaCl concentration was 1.0 M for all temperatures. Dry film thicknesses = 860 ± 80 nm. The fits for the semi-infinite equation are denoted by lines of the corresponding color using diffusion coefficients in **B**. The Arrhenius plot in **B** (*ln*D versus 1/T) yields activation energies above and below the glass transition of 53 and 98 kJ mol^{-1}, respectively.

Exchange of S-dPSS for S-hPSS was performed using the same range of temperatures (Figure 5). D for S-PSS was higher than D for L-PSS at comparable temperatures. Diffusion was again faster above T_g and near T_g dropped precipitously. E_a above T_g was 21 kJ mol^{-1} and could not be measured reliably below T_g The difference between E_a above T_g for L-PSS and S-PSS may be related to diffusion controlled respectively by entanglement/reptation and Rouse modes.[50] Previous studies have also shown that high molecular weight polyelectrolytes diffuse more slowly through PEMUs.[51] Yu et al. reported that diffusion of polyanions in exponentially growing films is slower with longer chains, indicated by slow initial buildup compared to lower molecular weight samples of the same polyelectrolytes.[52] They were able to obtain similar film thicknesses from different molecular weights by increasing exposure time for the high molecular weight films. This finding parallels the differences in exchange seen here between the L-PSS and S-PSS samples, with the L-PSS films requiring longer exposure time at the same temperatures to reach the same level of exchange as the S-PSS counterpart.

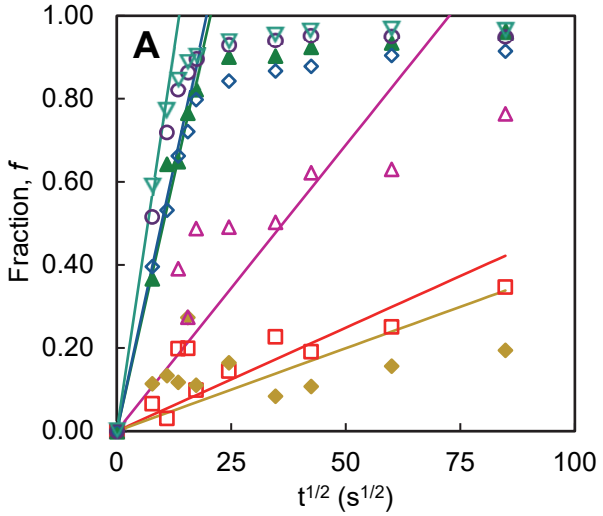

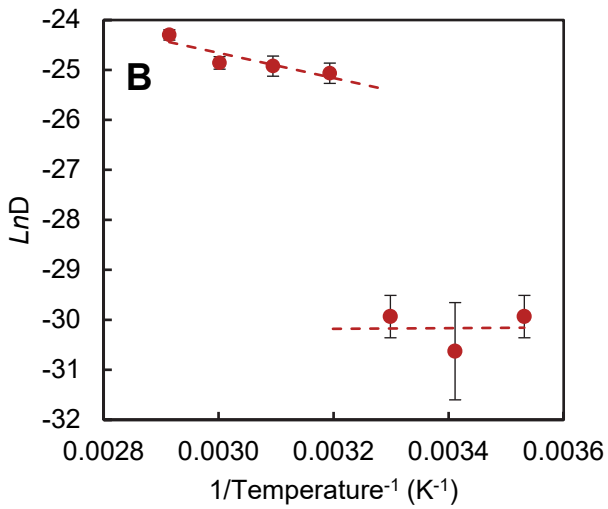

Figure 5. Exchange of S-dPSS with S-hPSS in a PDADMA/PSS PEMU with increasing temperature (**A**); 10 ºC (□), 20 ºC (♦), 30 ºC (Δ), 40 ºC (▲), 50ºC (◊), 60 ºC (○), and 70 ºC (▽). NaCl concentration was 1.0 M for all temperatures. Dry film thicknesses = 530 ± 60 nm. The fits for the semi-infinite equation are denoted by lines of the corresponding color. (**B**) Arrhenius plot of *ln*D (cm^2 s^{-1}) versus $temperature^{-1}$. The activation energy above the glass transition is 21 kJ mol^{-1}.

Dependence of D on [NaCl]

Many studies have illustrated the enhancement of polymer chain dynamics within complexed polyelectrolytes with an increase in salt concentration.[47, 53, 54] An equivalence or "superposition" of salt and temperature has been highlighted, where the acceleration of dynamics, for example in linear viscoelastic response, by temperature increases may be paralleled by an increase in salt concentration.[47, 55, 56, 57] The exchange of L-PSS and S-PSS in PEMUs at room temperature was monitored over a range of salt concentrations from 0.1 to 1.5 M NaCl. Figure 6 shows the L-PSS exchange data and their fit to the semi-infinite approximation in Equation 1. The data begins to deviate from Eq 1 at fraction less than 0.6, suggesting slower diffusion at later stages of the exchange.

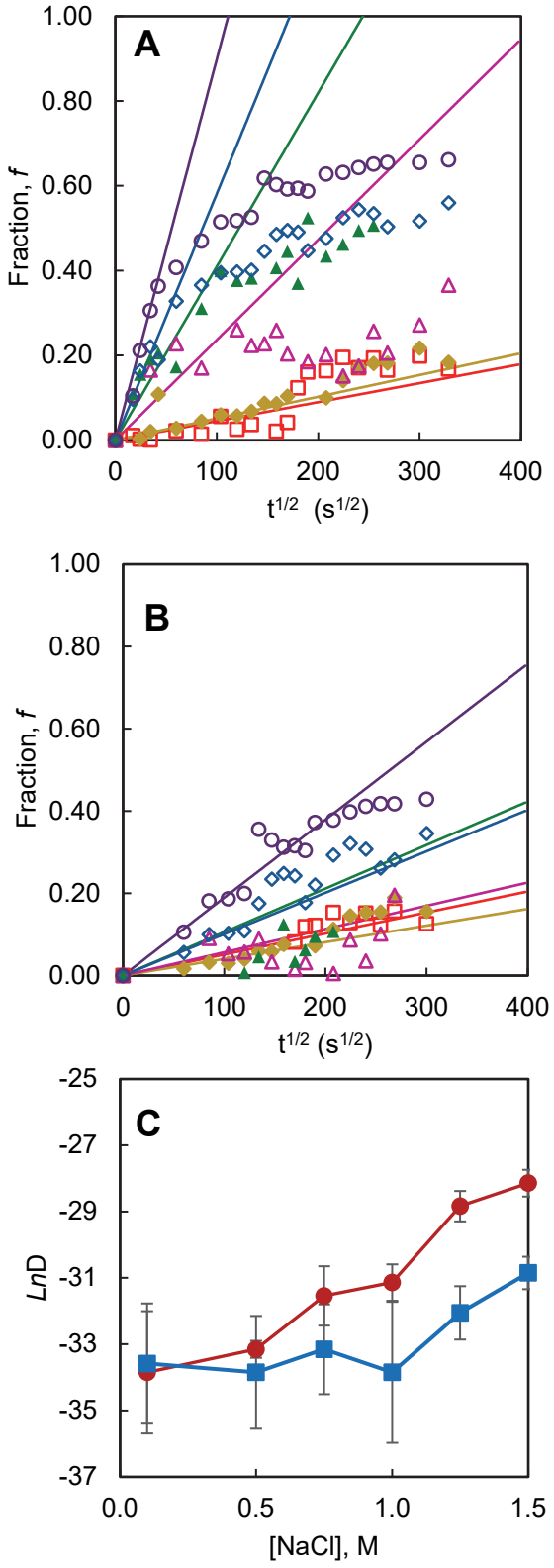

Figure 6: Exchange for L-PSS PEMU; D1 (A), D2 (B) components with increasing NaCl concentration, and the log of D1 and D2 ($cm^2\ s^{-1}$) versus salt concentration; 0.1 M (□), 0.5 M (♦),

0.75 M (△), 1.0 M (▲), 1.25 M (◊), and 1.5 M (○). All exchanges were conducted at room temp. Dry film thickness = 850 ± 40 nm. The semi-infinite fits are denoted by solid lines of the corresponding color (See Supporting Information Figure S10 for individual fits). (C); Diffusion coefficients D1 (●) and D2 (■) for L-PSS films at different concentrations of NaCl.

This apparent change in D was modeled by assuming that towards the PEMU/solution interface there is a stratum where the polymer diffuses faster (higher D, D1), illustrated in Scheme 2. At some depth, the molecules experience a second stratum of lower D (Scheme 2). Thus, the exchange experiment begins with typical behavior wherein f is linear with $t^{1/2}$. The lower region marks the start of a new f versus $t^{1/2}$ behavior with a lower D.

Figure 6B shows the data modeled using Equation 1 but with a second diffusion coefficient for the later time points (see the Supporting Information Table S1 for the points used to denote the start of the second, slower diffusion). Figure 6C shows the variation of D1 and D2 with [NaCl]. D1 and perhaps D2 do increase with increasing salt concentration, with a step-like increase from 1 to 1.25 M NaCl similar to the strong increase in layer-by-layer growth rate observed with the PDADMA/PSS system at this [NaCl].[1, 19]

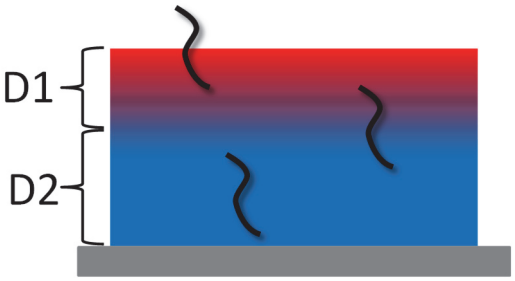

Scheme 2. Depiction of multilayer system with two regions of different diffusion coefficients. The red is rubbery and adjacent to the solution (providing faster diffusion, D1). The blue is glassy (D2).

The exchange rate for S-PSS as a function of [NaCl] was determined over the same [NaCl] range. Two strong differences between L-PSS and S-PSS may be observed with reference to Figure 7. Unlike L-PSS, the data for S-PSS were fit using a single diffusion coefficient. In addition, the diffusion coefficient showed no significant dependence on [NaCl] (Figure 7B). Comparing Figures 5 and 7, suggests there is no salt-temperature equivalence for short chains.

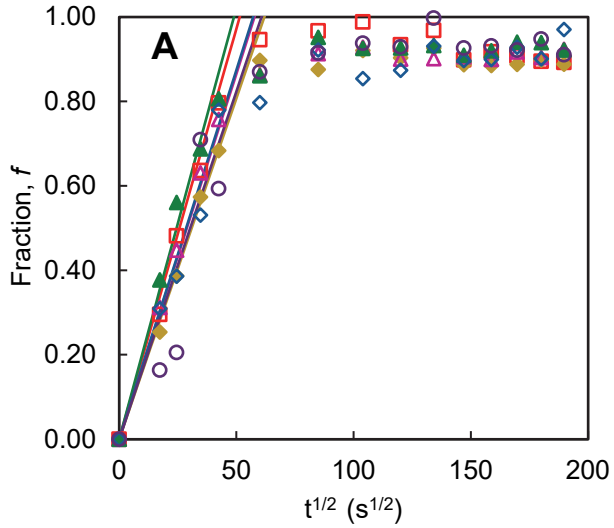

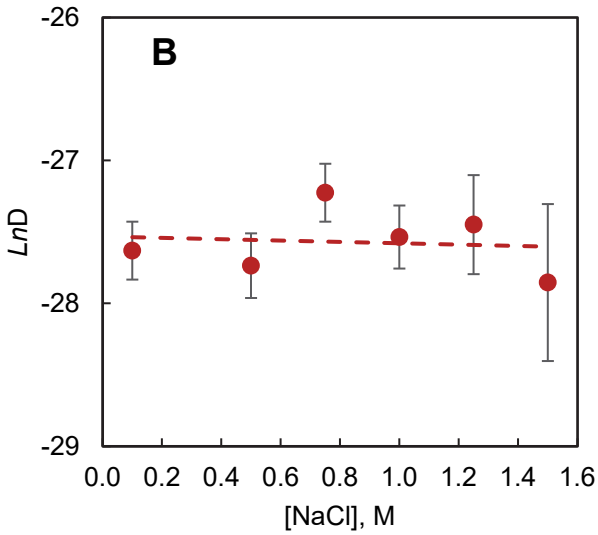

Figure 7. (A) Exchange for S-PSS PEMU with increasing [NaCl]: 0.1 M (□), 0.5 M (♦), 0.75 M (Δ), 1.0 M (▲), 1.25 M (◊), and 1.5 M (○). (B): *ln*D (D in cm^2 s^{-1}) versus salt concentration. Film thicknesses = 480 ± 60 nm. Experiments were performed at room temperature, (23 °C). The fits for the semi-infinite equation are denoted by lines of the corresponding color.

A single diffusion coefficient for short chains implies they do not experience different regions as shown in Scheme 2, probably because they are above their T_g throughout the film. Figure 3 shows a lower T_g for the short compared to the long hPSS chains. Interestingly, the T_g for the S-PSS PEC is lower though the PDADMA molecular weight is held constant. Studying the influence of the reversed combination (high molecular weight PSS complexed with short- *versus* long PDADMA chains) would provide information as to the relative contributions of the two polyelectrolytes to T_g.

The surface[58] and substrate[59] environments have each been suggested to influence properties of the multilayer system. For instance, the glass transition temperature (T_g) of polyelectrolyte multilayers is greatly affected by free volume[60] and water content. It has been suggested that the surface interactions between the surroundings and polyelectrolyte multilayers increase water content,[61, 62, 63] thereby decreasing the glass transition temperature at the surface of the film. It also has been suggested that there is an induced ordering by the substrate that increases the glass transition temperature of the section of the film closest to the substrate in polymeric thin films.[64, 65] Both scenarios imply there may a rubbery region and a glassy region coexisting within a single PEMU within a certain temperature range. The rate of diffusion through a polymer is temperature dependent, but it also is dependent upon whether the polymer is above or below the glass transition temperature. If there exists a two-region system, where part of the film is glassy, and the rest is rubbery, there would also be two different diffusion regimes through the film corresponding to those differences in moduli.

This multi-part diffusion for longer chain lengths is similar to what was seen by Porcel and coworkers when monitoring the diffusion of poly(l-lysine) (PLL) during the buildup of hyaluronic acid/poly(L-lysine) multilayers.[66] In that study, PLL of two molecular weights were tagged with a fluorescent marker and diffused through the films. The lower molecular weight sample was able to diffuse throughout the entire film, however as also seen in the current study the higher molecular weight sample experienced fast then slow diffusion. Xu et al., showed that polyelectrolyte diffusion in poly(2-(dimethylamino)-ethyl methacrylate)/poly(methacrylic acid) scaled approximately with M_w^{-1}.[51] Kienle and Schwartz studied the salt dependence of PLL diffusion in PLL/poly(2-acrylamido-2-methyl-1-propanesulfonic acid) and saw an increase in diffusion coefficient with increasing salt ranging from 0 - 1.5 M NaCl, as well as noting the subdiffusive nature of the films (not obeying truly random Brownian motion) for short time.[67]

A series of thickness and diffusion studies were performed to delve further into the idea of a multi-step diffusion regime shown in Figure 6. The thickness of the film changes the T_g through interactions either with the surface or with the substrate. Which interface influences T_g can be determined by monitoring the slowdown of the diffusion data as it changes with the thickness of the films. For the L-PSS system three films were analyzed: 60-, 40-, or 20 layers thick. If the exchange slows at lower fractions of exchange with increased film thickness, it indicates that surface interactions are dominant. This is because surface interactions can only penetrate to a certain depth into the film, and that depth is not dependent on the film thickness. If substrate interactions are dominant, exchange in the thicker films would slow at higher fractions (Scheme 3).

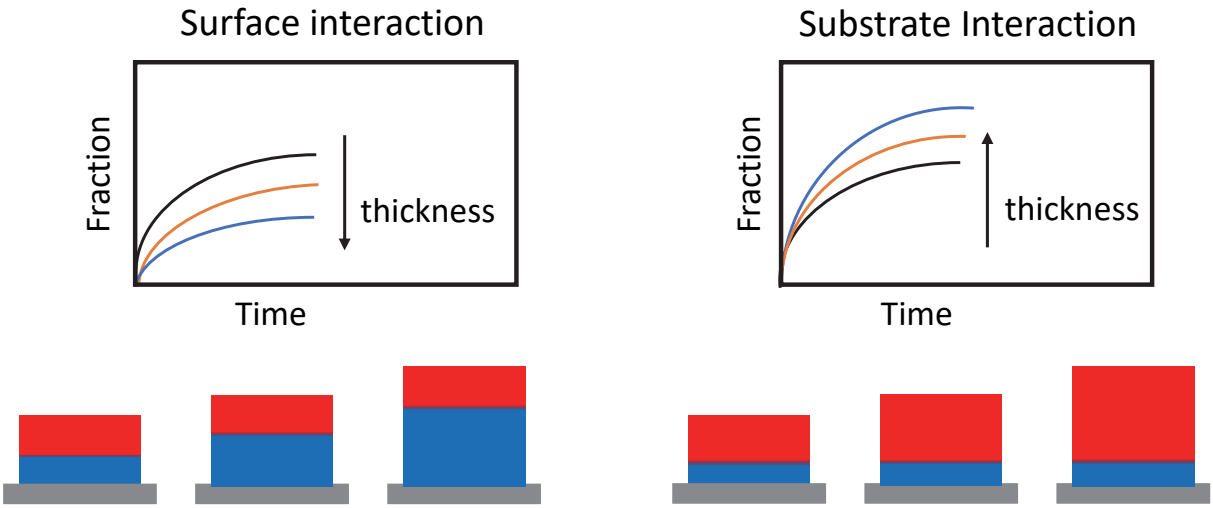

Scheme 3. Showing how PSS exchange rate depends on film thickness if dominated by surface interactions (left) or substrate interactions (right). Diffusion in red strata is faster than in blue.

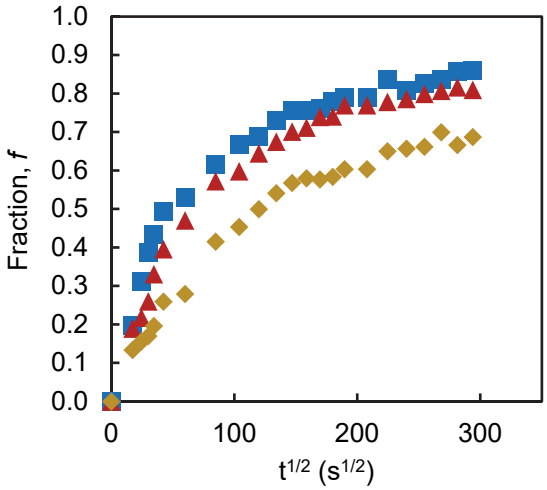

Figure 8. Normalized dPSS/1185 cm^{-1} peak area ratio for L-PSS PEMUs with 20 (■), 40 (▲), and 60 (♦) layers to compare how thickness affects the degree of exchange for comparison with Scheme 3. Temperature was 25 ºC and [NaCl] was 1.5 M.

Figure 8 shows the plateaus for the three films analyzed. The fraction of exchanged polymer slows with increasing film thickness, indicating that surface interactions are dominating.

This is aligned with findings by Tanchak et al., showing that towards the surface of PEMUs there is an increase in water content.[61] T_g for these systems decreases with increasing water content, so the higher water content at the surface provides a lower T_g at the surface, allowing faster diffusion.[60]

Conclusions

This comparison of the diffusion of short and long chains of narrow molecular weight distribution PSS through films of polyelectrolyte complex revealed some surprising differences in response to salt concentration and temperature. Because the T_g of PDADMA/PSS PEC is close to room temperature, additional sensitivity to these two parameters was observed. For the two lengths of PSS, one believed to be below and one above the entanglement threshold, a change in diffusion coefficient was observed near T_g, though D was generally much higher for the shorter chain. The activation energy above T_g for long chains was about 53 kJ mol^{-1}, similar to the activation energy for the rearrangement of two pairs of Pol^+Pol^-, and was about 21 kJ mol^{-1} for short chains. The diffusion of S-PSS at room temperature was not sensitive to salt concentration, probably because the PEMU made with S-PSS is below the T_g at room temperature, whereas L-PSS exhibited an increase in D at conditions near the glass transition. The importance of the relationship between materials properties and T_g was further illustrated by the observation that the mobility of L-PSS was greater near the surface of the film, which correlated with a lower T_g in that region induced by a greater degree of hydration. These studies emphasize the need to know whether the material is above T_g when making measurements of polymer diffusion in PECs. As far as is known to date, all fully hydrated PECs containing polycarboxylates are above T_g at room temperature, whereas PECs with PSS may not be. Since many potential applications of PECs employ the PEMU or ultrathin films morphology, for example, as membranes or coatings, the resilience of these coatings depends strongly on whether they are below or above T_g.

Supporting Information

Starting fraction for D2; table of diffusion coefficients; FT-IR comparison of deuterated multilayer and protiated multilayers; FT-IR spectral stacks; normalized dPSS/1185 cm^{-1} peak area ratios; graphical breakdown of D1 and D2; rheological data for long and short chains.

Authors

ORCID IDs

Rachel L Abbett: 0000-0002-4019-4925

Yuhui Chen: 0000-0002-5416-2350

Joseph B. Schlenoff: 0000-0001-5588-1253

Notes

The authors declare no competing financial interest.

Acknowledgement

This work was supported by a grant from the National Science Foundation DMR-1809304.

References

1. Dubas, S. T.; Schlenoff, J. B. Factors Controlling the Growth of Polyelectrolyte Multilayers. *Macromolecules* **1999,** *32*, 8153-8160.
2. Schönhoff, M. Self-Assembled Polyelectrolyte Multilayers. *Current Opinion in Colloid & Interface Science* **2003,** *8*, 86-95.
3. Marciel, A. B.; Srivastava, S.; Tirrell, M. V. Structure and Rheology of Polyelectrolyte Complex Coacervates. *Soft Matter* **2018,** *14*, 2454-2464.
4. Owusu-Nkwantabisah, S.; Gammana, M.; Tripp, C. P. Dynamics of Layer-by-Layer Growth of a Polyelectrolyte Multilayer Studied in Situ Using Attenuated Total Reflectance Infrared Spectroscopy. *Langmuir* **2014,** *30*, 11696-703.
5. Picart, C.; Mutterer, J.; Richert, L.; Luo, Y.; Prestwich, G. D.; Schaaf, P.; Voegel, J. C.; Lavalle, P. Molecular Basis for the Explanation of the Exponential Growth of Polyelectrolyte Multilayers. *Proc Natl Acad Sci U S A* **2002,** *99*, 12531-5.
6. Hübsch, E.; Ball, V.; Senger, B.; Decher, G.; Voegel, J.-C.; Schaaf, P. Controlling the Growth Regime of Polyelectrolyte Multilayer Films: Changing from Exponential to Linear Growth by Adjusting the Composition of Polyelectrolyte Mixtures. *Langmuir* **2004,** *20*, 1980-1985.
7. Schmitt, J.; Grünewald, T.; Decher, G.; Pershan, P. S.; Kjaer, K.; Lösche, M. Internal Structure of Layer-by-Layer Adsorbed Polyelectrolyte Films: A Neutron and X-Ray Reflectivity Study. *Macromolecules* **1993,** *26*, 7058-7063.
8. Salomäki, M.; Tervasmäki, P.; Areva, S.; Kankare, J. The Hofmeister Anion Effect and the Growth of Polyelectrolyte Multilayers. *Langmuir* **2004,** *20*, 3679-3683.
9. Decher, G. Fuzzy Nanoassemblies: Toward Layered Polymeric Multicomposites. *Science* **1997,** *277*, 1232-1237.
10. Ghostine, R. A.; Markarian, M. Z.; Schlenoff, J. B. Asymmetric Growth in Polyelectrolyte Multilayers. *Journal of the American Chemical Society* **2013,** *135*, 7636-7646.
11. Boudou, T.; Crouzier, T.; Ren, K.; Blin, G.; Picart, C. Multiple Functionalities of Polyelectrolyte Multilayer Films: New Biomedical Applications. **2010,** *22*, 441-467.
12. Labala, S.; Mandapalli, P. K.; Kurumaddali, A.; Venuganti, V. V. K. Layer-by-Layer Polymer Coated Gold Nanoparticles for Topical Delivery of Imatinib Mesylate to Treat Melanoma. *Molecular Pharmaceutics* **2015,** *12*, 878-888.
13. Guillaume-Gentil, O.; Akiyama, Y.; Schuler, M.; Tang, C.; Textor, M.; Yamato, M.; Okano, T.; Vörös, J. Polyelectrolyte Coatings with a Potential for Electronic Control and Cell Sheet Engineering. **2008,** *20*, 560-565.
14. Lutkenhaus, J. L.; Hammond, P. T. Electrochemically Enabled Polyelectrolyte Multilayer Devices: From Fuel Cells to Sensors. *Soft Matter* **2007,** *3*, 804-816.
15. Hsiao, Y.-S.; Whang, W.-T.; Chen, C.-P.; Chen, Y.-C. High-Conductivity Poly(3,4-Ethylenedioxythiophene):Poly(Styrene Sulfonate) Film for Use in ITO-Free Polymer Solar Cells. *Journal of Materials Chemistry* **2008,** *18*, 5948-5955.
16. Tou, Z. Q.; Chan, C. C.; Leong, S. A Fiber-Optic pH Sensor Based on Polyelectrolyte Multilayers Embedded with Gold Nanoparticles. *Measurement Science and Technology* **2014,** *25*, 075102.
17. te Brinke, E.; Achterhuis, I.; Reurink, D. M.; de Grooth, J.; de Vos, W. M. Multiple Approaches to the Buildup of Asymmetric Polyelectrolyte Multilayer Membranes for Efficient Water Purification. *ACS Applied Polymer Materials* **2020,** *2*, 715-724.
18. Fares, H. M.; Schlenoff, J. B. Equilibrium Overcompensation in Polyelectrolyte Complexes. *Macromolecules* **2017,** *50*, 3968-3978.
19. Guzmán, E.; Ritacco, H.; Rubio, J. E. F.; Rubio, R. G.; Ortega, F. Salt-Induced Changes in the Growth of Polyelectrolyte Layers of Poly(Diallyl-Dimethylammonium Chloride) and Poly(4-Styrene Sulfonate of Sodium). *Soft Matter* **2009,** *5*, 2130.
20. Hoogeveen, N. G.; Cohen Stuart, M. A.; Fleer, G. J.; Böhmer, M. R. Formation and Stability of Multilayers of Polyelectrolytes. *Langmuir* **1996,** *12*, 3675-3681.
21. Han, L.; Mao, Z.; Wuliyasu, H.; Wu, J.; Gong, X.; Yang, Y.; Gao, C. Modulating the Structure and Properties of Poly(Sodium 4-Styrenesulfonate)/Poly(Diallyldimethylammonium Chloride) Multilayers with Concentrated Salt Solutions. *Langmuir* **2012,** *28*, 193-199.

22. Kovačević, D.; Van der Burgh, S.; de Keizer, A.; Cohen Stuart, M. A. Kinetics of Formation and Dissolution of Weak Polyelectrolyte Multilayers: Role of Salt and Free Polyions. *Langmuir* **2002,** *18*, 5607-5612.
23. Lösche, M.; Schmitt, J.; Decher, G.; Bouwman, W. G.; Kjaer, K. Detailed Structure of Molecularly Thin Polyelectrolyte Multilayer Films on Solid Substrates as Revealed by Neutron Reflectometry. *Macromolecules* **1998,** *31*, 8893-8906.
24. Michaels, A. S. Polyelectrolyte Complexes. *Industrial & Engineering Chemistry* **1965,** *57*, 32-40.
25. Xu, L.; Kozlovskaya, V.; Kharlampieva, E.; Ankner, J. F.; Sukhishvili, S. A. Anisotropic Diffusion of Polyelectrolyte Chains within Multilayer Films. *ACS Macro Letters* **2012,** *1*, 127-130.
26. Soltwedel, O.; Ivanova, O.; Nestler, P.; Müller, M.; Köhler, R.; Helm, C. A. Interdiffusion in Polyelectrolyte Multilayers. *Macromolecules* **2010,** *43*, 7288-7293.
27. Jomaa, H. W.; Schlenoff, J. B. Salt-Induced Polyelectrolyte Interdiffusion in Multilayered Films: A Neutron Reflectivity Study. *Macromolecules* **2005,** *38*, 8473-8480.
28. Fares, H. M.; Schlenoff, J. B. Diffusion of Sites Versus Polymers in Polyelectrolyte Complexes and Multilayers. *Journal of the American Chemical Society* **2017,** *139*, 14656-14667.
29. Zan, X.; Hoagland, D. A.; Wang, T.; Peng, B.; Su, Z. Polyelectrolyte Uptake by PEMs: Impacts of Molecular Weight and Counterion. *Polymer* **2012,** *53*, 5109-5115.
30. Feldötö, Z.; Varga, I.; Blomberg, E. Influence of Salt and Rinsing Protocol on the Structure of PAH/PSS Polyelectrolyte Multilayers. *Langmuir* **2010,** *26*, 17048-17057.
31. Sivaniah, E.; Sferrazza, M.; Jones, R. A. L.; Bucknall, D. G. Chain Confinement Effects on Interdiffusion in Polymer Multilayers. *Physical Review E* **1999,** *59*, 885-888.
32. Sill, A.; Nestler, P.; Azinfar, A.; Helm, C. A. Tailorable Polyanion Diffusion Coefficient in LbL Films: The Role of Polycation Molecular Weight and Polymer Conformation. *Macromolecules* **2019,** *52*, 9045-9052.
33. Sukhishvili, S. A.; Kharlampieva, E.; Izumrudov, V. Where Polyelectrolyte Multilayers and Polyelectrolyte Complexes Meet. *Macromolecules* **2006,** *39*, 8873-8881.
34. Selin, V.; Ankner, J. F.; Sukhishvili, S. A. Nonlinear Layer-by-Layer Films: Effects of Chain Diffusivity on Film Structure and Swelling. *Macromolecules* **2017,** *50*, 6192-6201.
35. Markarian, M. Z.; Hariri, H. H.; Reisch, A.; Urban, V. S.; Schlenoff, J. B. A Small-Angle Neutron Scattering Study of the Equilibrium Conformation of Polyelectrolytes in Stoichiometric Saloplastic Polyelectrolyte Complexes. *Macromolecules* **2012,** *45*, 1016-1024.
36. Lavalle, P.; Vivet, V.; Jessel, N.; Decher, G.; Voegel, J.-C.; Mesini, P. J.; Schaaf, P. Direct Evidence for Vertical Diffusion and Exchange Processes of Polyanions and Polycations in Polyelectrolyte Multilayer Films. *Macromolecules* **2004,** *37*, 1159-1162.
37. Lavalle, P.; Picart, C.; Mutterer, J.; Gergely, C.; Reiss, H.; Voegel, J.-C.; Senger, B.; Schaaf, P. Modeling the Buildup of Polyelectrolyte Multilayer Films Having Exponential Growth. *The Journal of Physical Chemistry B* **2004,** *108*, 635-648.
38. Richert, L.; Arntz, Y.; Schaaf, P.; Voegel, J.-C.; Picart, C. Ph Dependent Growth of Poly(L-Lysine)/Poly(L-Glutamic) Acid Multilayer Films and Their Cell Adhesion Properties. *Surface Science* **2004,** *570*, 13-29.
39. Schneider, A.; Francius, G.; Obeid, R.; Schwinté, P.; Hemmerlé, J.; Frisch, B.; Schaaf, P.; Voegel, J.-C.; Senger, B.; Picart, C. Polyelectrolyte Multilayers with a Tunable Young's Modulus: Influence of Film Stiffness on Cell Adhesion. *Langmuir* **2006,** *22*, 1193-1200.
40. Köhler, K.; Möhwald, H.; Sukhorukov, G. B. Thermal Behavior of Polyelectrolyte Multilayer Microcapsules: 2. Insight into Molecular Mechanisms for the PDADMAC/PSS System. *The Journal of Physical Chemistry B* **2006,** *110*, 24002-24010.
41. Shamoun, R. F.; Hariri, H. H.; Ghostine, R. A.; Schlenoff, J. B. Thermal Transformations in Extruded Saloplastic Polyelectrolyte Complexes. *Macromolecules* **2012,** *45*, 9759-9767.
42. Chen, Y.; Yang, M.; Schlenoff, J. B. Glass Transitions in Hydrated Polyelectrolyte Complexes. *Macromolecules* **2021,** *54*, 3822-3831.
43. Shaheen, S. A.; Yang, M.; Chen, B.; Schlenoff, J. B. Water and Ion Transport through the Glass Transition in Polyelectrolyte Complexes. *Chemistry of Materials* **2020,** *32*, 5994-6002.
44. Schlenoff, J. B.; Akkaoui, K. Dissecting Dynamics near the Glass Transition Using Polyelectrolyte Complexes. *Macromolecules* **2021,** *54*, 3413-3422.
45. Coughlin, J. E.; Reisch, A.; Markarian, M. Z.; Schlenoff, J. B. Sulfonation of Polystyrene: Toward the "Ideal" Polyelectrolyte. *J Polym Sci Pol Chem* **2013,** *51*, 2416-2424.

46. Shamoun, R. F.; Reisch, A.; Schlenoff, J. B. Extruded Saloplastic Polyelectrolyte Complexes. *Advanced Functional Materials* **2012,** *22*, 1923-1931.
47. Yang, M.; Shi, J.; Schlenoff, J. B. Control of Dynamics in Polyelectrolyte Complexes by Temperature and Salt. *Macromolecules* **2019,** *52*, 1930-1941.
48. Yang, J. C.; Jablonsky, M. J.; Mays, J. W. NMR and FT-IR Studies of Sulfonated Styrene-Based Homopolymers and Copolymers. *Polymer* **2002,** *43*, 5125-5132.
49. Crank, J. *The Mathematics of Diffusion*; Clarendon Press: Oxford, UK, 1975.
50. Akkaoui, K.; Yang, M.; Digby, Z. A.; Schlenoff, J. B. Ultraviscosity in Entangled Polyelectrolyte Complexes and Coacervates. *Macromolecules* **2020,** *53*, 4234-4246.
51. Xu, L.; Selin, V.; Zhuk, A.; Ankner, J. F.; Sukhishvili, S. A. Molecular Weight Dependence of Polymer Chain Mobility within Multilayer Films. *ACS Macro Letters* **2013,** *2*, 865-868.
52. Yu, J.; Meharg, B. M.; Lee, I. Adsorption and Interlayer Diffusion Controlled Growth and Unique Surface Patterned Growth of Polyelectrolyte Multilayers. *Polymer* **2017,** *109*, 297-306.
53. Saikaew, R.; Meesorn, W.; Zoppe, J. O.; Weder, C.; Dubas, S. T. Influence of the Salt Concentration on the Properties of Salt-Free Polyelectrolyte Complex Membranes. *Macromolecular Materials and Engineering* **2019,** *304*, 1900245.
54. Morin, F. J.; Puppo, M. L.; Laaser, J. E. Decoupling Salt- and Polymer-Dependent Dynamics in Polyelectrolyte Complex Coacervates Via Salt Addition. *Soft Matter* **2021,** *17*, 1223-1231.
55. Ali, S.; Prabhu, V. Relaxation Behavior by Time-Salt and Time-Temperature Superpositions of Polyelectrolyte Complexes from Coacervate to Precipitate. *Gels* **2018,** *4*, 11.
56. Spruijt, E.; Sprakel, J.; Lemmers, M.; Stuart, M. A. C.; van der Gucht, J. Relaxation Dynamics at Different Time Scales in Electrostatic Complexes: Time-Salt Superposition. *Physical Review Letters* **2010,** *105*, 208301.
57. Liu, Y.; Momani, B.; Winter, H. H.; Perry, S. L. Rheological Characterization of Liquid-to-Solid Transitions in Bulk Polyelectrolyte Complexes. *Soft Matter* **2017,** *13*, 7332-7340.
58. Zerball, M.; Laschewsky, A.; von Klitzing, R. Swelling of Polyelectrolyte Multilayers: The Relation between, Surface and Bulk Characteristics. *The Journal of Physical Chemistry B* **2015,** *119*, 11879-11886.
59. Buron, C. C.; Filiâtre, C.; Membrey, F.; Bainier, C.; Charraut, D.; Foissy, A. Effect of Substrate on the Adsorption of Polyelectrolyte Multilayers: Study by Optical Fixed-Angle Reflectometry and AFM. *Colloids and Surfaces A: Physicochemical and Engineering Aspects* **2007,** *305*, 105-111.
60. Zhang, Y.; Batys, P.; O'Neal, J. T.; Li, F.; Sammalkorpi, M.; Lutkenhaus, J. L. Molecular Origin of the Glass Transition in Polyelectrolyte Assemblies. *ACS Central Science* **2018,** *4*, 638-644.
61. Tanchak, O. M.; Yager, K. G.; Fritzsche, H.; Harroun, T.; Katsaras, J.; Barrett, C. J. Water Distribution in Multilayers of Weak Polyelectrolytes. *Langmuir* **2006,** *22*, 5137-5143.
62. Ghoussoub, Y. E.; Zerball, M.; Fares, H. M.; Ankner, J. F.; von Klitzing, R.; Schlenoff, J. B. Ion Distribution in Dry Polyelectrolyte Multilayers: A Neutron Reflectometry Study. *Soft Matter* **2018,** *14*, 1699-1708.
63. Tanchak, O. M.; Yager, K. G.; Fritzsche, H.; Harroun, T.; Katsaras, J.; Barrett, C. J. Ion Distribution in Multilayers of Weak Polyelectrolytes: A Neutron Reflectometry Study. *The Journal of Chemical Physics* **2008,** *129*, 084901.
64. Torres, J. A.; Nealey, P. F.; de Pablo, J. J. Molecular Simulation of Ultrathin Polymeric Films near the Glass Transition. *Physical Review Letters* **2000,** *85*, 3221-3224.
65. Ellison, C. J.; Torkelson, J. M. The Distribution of Glass-Transition Temperatures in Nanoscopically Confined Glass Formers. *Nat Mater* **2003,** *2*, 695-700.
66. Porcel, C.; Lavalle, P.; Decher, G.; Senger, B.; Voegel, J. C.; Schaaf, P. Influence of the Polyelectrolyte Molecular Weight on Exponentially Growing Multilayer Films in the Linear Regime. *Langmuir* **2007,** *23*, 1898-1904.
67. Kienle, D. F.; Schwartz, D. K. Complex Salt Dependence of Polymer Diffusion in Polyelectrolyte Multilayers. *J Phys Chem Lett* **2019,** *10*, 987-992.